Langmuir
Letter
pubs.acs.org/Langmuir
© 2009 American Chemical Society

# Selective Nanofiber Deposition Using a Microfluidic Confinement Approach

Haifeng Yang and Liang Dong*

*Department of Electrical and Computer Engineering, Iowa State University, Ames, Iowa 50011*

*Received October 20, 2009. Revised Manuscript Received December 8, 2009*

The ability to create structurally complex, accurate micropatterns in biocompatible and biodegradable nanofiber mats is important in maximally mimicking the natural extracellular matrix (ECM) for cell biology and tissue engineering. We present a simple, versatile method for the selective deposition of nanofibers with high definition using a unique microfluidic fiber collector. The collector contains fiber etching solutions that are selectively confined to defined regions by means of photocleavable self-assembled monolayer technology and microfluidic capillary filling. The presented approach achieves arbitrarily shaped, microsized, structurally accurate architectures in both random and aligned nanofibers.

## Introduction

Electrospinning is an economical, versatile technique used to fabricate continuous nanofibers.[1] The basic principle of electrospinning is that a Taylor cone of a polymer solution is formed at the tip of a metallic spinneret by applying high voltage between the spinneret and a grounded collector. When the electrostatic repulsion in the polymer solution overcomes the surface tension, a charged fluid jet is ejected out of the spinneret, traveling through the air with solvent evaporation. Finally, nanofibers are deposited on the collector. A number of polymeric, metallic, and ceramic nanofibers have been realized through electrospinning.[2,3] Among them, electrospun nanofiber biomaterials possess highly porous structures with numerous interconnected nanopores resembling the architecture of natural ECM. Consequently, nanofiber-based artificial ECM scaffolds have attracted much attention and have shown great promises in musculoskeletal, skin, vascular, and neural tissue engineering applications, where they serve as excellent frameworks to improve cell adhesion, proliferation, and differentiation.[4−10]

To maximally mimic natural ECM scaffolds, it is crucial to develop the ability to create structurally complex, high-definition shapes of nanofibers. For example, research on regenerative medicine has revealed that tissue formation relies considerably on the spatial orientation and distribution of scaffolds that control and guide cell growth and proliferation.[11] However, achieving structurally accurate, arbitrarily shaped micropatterns of nanofibers remains a challenge. Current research on this topic is carried out in three major areas. The first area is controlling the spatial orientation of nanofibers on collectors by overcoming the random deposition process of conventional electrospinning.[12−22] In this area, nanofiber alignment has been successfully accomplished by manipulating the applied electrostatic field through various modifications to fiber collectors, including using paired conductive silicon strips separated by a void gap,[12] multiple metal electrodes with particular configurations formed on an insulting substrate,[13] and two pieces of conductive blades placed in line with a gap in between.[14] Other interesting fiber alignment strategies include using a rotating collection drum,[15,16] a wheel-like bobbin or metal frame,[15,17] and near-field electrospinning.[18] The second area aims at forming patterned electrospun mats to achieve the controlled spatial distribution of nanofibers. To this end, many important and promising technologies have been reported. For example, conductive collectors with insulating regions of different areas and geometric shapes,[19] woven wire fabric substrates,[20] and enamel-coated steel sheets[21] have been employed to obtain nanofiber mats with various patterned architectures. The third area involves the selective deposition of nanofibers in discrete regions on collectors.[22−28] In this area, the controlled mechanical movement of a collector during electrospinning has provided a straightforward approach to the discrete

*Author to whom correspondence should be addressed. E-mail: ldong@iastate.edu. Phone: 515-294-0388. Fax: 515-294-8432.

(1) Li, D.; Xia, Y. *Adv. Mater.* **2004**, *16*, 1151–1170.
(2) Bognitzki, B.; Becker, M.; Graeser, M.; Massa, W.; Wendorff, J. H.; Schaper, A.; Weber, D.; Beyer, A.; Golzhauser, A; Greiner, A. J. *Adv. Mater.* **2006**, *18*, 2384–2386.
(3) Li, D.; McCann, J.; Xia, Y. *J. Am. Ceram. Soc.* **2006**, *89*, 1861–1869.
(4) Min, B.; Lee, G.; Kin, S. H.; Nam, Y. S.; Lee, T. S.; Park, W. H. *Biomaterials* **2004**, *25*, 1289–1297.
(5) Yang, F.; Murugan, R.; Wang, S.; Ramakrishna, S. *Biomaterials* **2005**, *26*, 2603–2610.
(6) Choi, J. S.; Lee, S. J.; Christ, G. J.; Atala, A.; Yoo, J. J. *Biomaterials* **2008**, *29*, 2899–2906.
(7) Wnek, G. E.; Carr, M. E.; Simpson, D. G.; Bowlin, G. L. *Nano Lett.* **2003**, *3*, 213–216.
(8) Zhu, X.; Cui, W.; Li, X.; Jin, Y. *Biomacromolecules* **2008**, *9*, 1795–1801.
(9) Srouji, S.; Kizhner, T.; Suss-Tobi, E.; Livne, E.; Zussman, E. *J. Mater. Sci: Mater. Med.* **2008**, *19*, 1249–1255.
(10) Townsend-Nicholson, A.; Jayasinghe, S. N. *Biomacromolecules* **2006**, *7*, 3364–3369.
(11) Recknor, J. B.; Sakaguchi, D. S.; Mallapragada, S. K. *Biomaterials* **2006**, *27*, 4098–4108.
(12) Li, D.; Wang, Y.; Xia, Y. *Nano Lett.* **2003**, *3*, 1167–1171.
(13) Li, D.; Wang, Y.; Xia, Y. *Adv. Mater.* **2004**, *16*, 361–366.
(14) Teo, W. E.; Ramakrishna, S. *Nanotechnology* **2005**, *16*, 1878–1884.
(15) Huang, Z. M.; Zhang, Y. Z.; Kotaki, M.; Ramakrishna, S. *Compos. Sci. Technol.* **2003**, *63*, 2223–2253.
(16) Doshi, J.; Reneker, D. H. *J. Electrost.* **1995**, *35*, 151–160.
(17) Theron, A.; Zussman, E.; Yarin, A. L. *Nanotechnology* **2001**, *12*, 384–390.
(18) Sun, D.; Chang, C.; Li, S.; Lin, L. *Nano Lett.* **2006**, *6*, 839–842.
(19) Li, D.; Ouyang, M.; McCann, J. T.; Xia, Y. *Nano Lett.* **2005**, *5*, 913–916.
(20) Zhang, D.; Chang, J. *Adv. Mater.* **2007**, *19*, 3664–3667.
(21) Zucchelli, A.; Fabiani, D.; Gualandi, C.; Focarete, M. *J. Mater. Sci.* **2009**, *44*, 4969–4975.
(22) Ding, Z.; Salim, A.; Ziaie, B. *Langmuir* **2009**, *25*, 9648–9652.
(23) Dalton, P. D.; Joergensen, N. T.; Groll, J.; Moeller, M. *Biomed. Mater.* **2008**, *3*, 034109.
(24) Ikeuchi, M.; Tane, R.; Fukuoka, M.; Ikuta, K. *IEEE 22nd Int. Conf. Micro Electro Mech. Syst.* **2009**, 124–127.
(25) Salim, A.; Son, C.; Ziaie, B. *Nanotechnology* **2008**, *19*, 375303.
(26) Shi, J.; Wang, L.; Chen, Y. *Langmuir* **2009**, *25*, 6015–6018.
(27) Zeng, H.; Zhao, Y. *15th Int. Conf. Solid-State Sens. Actuators Microsyst.* **2009**, 1099–1103.
(28) Choi, H. W.; Johnson, J. K.; Nam, J.; Farson, D. F. *J. Laser Appl.* **2007**, *19*, 225–231.

placement of nanofibers.[23] The resulting patterns, however, have poorly defined shapes with feature sizes on the order of hundreds of micrometers to a few millimeters. Recently, electrodynamic focusing of nanofibers has been demonstrated to achieve microspots of nonwoven nanofibers on a collector, but this technology requires a secondary electric field created by a specially designed electrostatic lens[24] or a metal-coated shadow mask.[25] Shi et al. used conventional photolithography to form discrete nanofiber patterns. However, it remains challenging to maintain the morphological appearance and material properties of electrospun mats after multiple processing steps (spin coating of photoresist, soft baking, exposure, development, dry/wet etching).[26] Other technologies in this area include using electrical discharge[27] and femtosecond laser micromachining.[28] In this letter, we present a simple and versatile method for the selective deposition of nanofibers using a unique microfluidic collector, allowing the formation of high-definition patterns of nanofibers on a glass substrate for cell biology and tissue engineering. This research falls in the third area mentioned above.

## Concept of Microfluidic Patterning of Electrospun Fibers

Figure 1 illustrates the basic principle and process of the proposed selective nanofiber deposition technology. The method is to selectively pattern the affinity of different regions of the collector surface for a water-containing fiber-etching solution. The nanofiber deposition region is hydrophobic and repels the etching solution; its peripheral region is hydrophilic and attracts the etching solution (Figure 1a). These two regions are prepatterned by means of photocleavable self-assembled monolayer (SAM) technology that allows the transfer of hydrophobic and hydrophilic patterns from a photomask to the collector surface (described in the Experimental Section).[30] The fiber-etching solution used here is either pure water or a mixture of water and a suitable organic solvent that is fully miscible with water or has an acceptable solubility in water (SW). The water-containing etching solution is allowed to flow into the hydrophilic region through a microfluidic capillary filling process and is stably confined there without crossing the hydrophilic−hydrophobic line (Figure 1b). Therefore, a unique microfluidic collector is formed, where the hydrophobic (dry) region is separated from the hydrophilic (wet) region. During electrospinning, fibers pile up on the dry surface and dissolve in the etching solution confined to the wet region (Figure 1c,d). Finally, the remaining polymer residues from the etching process are washed away from the wet surface by fresh etching solution, leaving nanofibers only in the dry region (Figure 1e,f). In this method, the shape definition of the deposited nanofibers is determined by the patterns on the photomask and by the lateral overetch that occurs at the edges of the nanofiber patterns (details in the Results and Discussion section). Therefore, it is possible to form arbitrary nanofiber shapes simply by designing the patterns of the photomask. It should also be noted that because a rather wide variety of organic solvents are available to mix with water to obtain the proper water-containing etching solution (described in the Results and Discussion section) the presented selective nanofiber deposition technology can be applied to a broad range of nanofiber biomaterials.

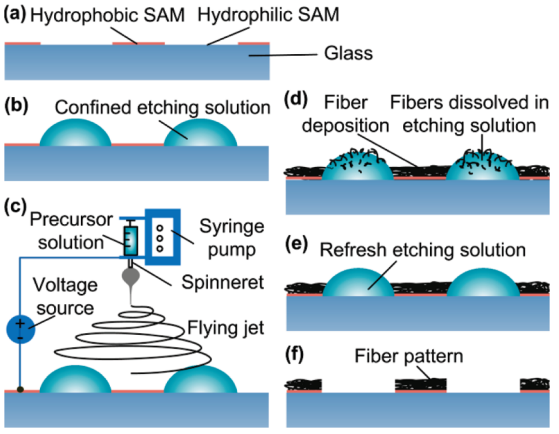


**Figure 1.** Principle and process of selective nanofiber deposition using a microfluidic collector. (a) The hydrophilic and hydrophobic regions are selectively patterned onto the collector surface using photocleavable SAM technology. (b) The water-containing etching solution flows into the hydrophilic region via microfluidic filling and is confined to that region because of the surrounding hydrophobic surface. (c) The nanofibers are deposited onto the microfluidic collector using electrospinning. (d) The etching solution dissolves the nanofibers in the hydrophilic region. (e) The polymer residues from the etching process are washed away by flowing fresh etching solution into the hydrophilic region. (f) The nanofibers are selectively deposited onto the hydrophobic region of the collector surface.

## Experimental Section

**Materials.** Two typical biomaterials are used to demonstrate the method: water-soluble polyethylene oxide (PEO) and water-insoluble poly-DL-lactic acid (PDLLA). PEO (MW = 1 000 000), chloroform (HPLC grade, 99.9%), fluorescein (pure, MW = 332.3), and ethanol (100%) were obtained from Sigma-Aldrich (St. Louis, MO). Hydrofluoric acid (49 w/w %) and acetone were obtained from Fisher Scientific (Pittsburgh, PA). PDLLA (i.v. = 0.69) was obtained from Lactel Polymers (Birmingham, AL). All reagents were used as received without further purification.

**Precursor Preparation.** The PEO precursor is prepared by dissolving PEO powder in 70% (V/V) ethanol (diluted with deionized water) with a weight ratio of 0.3:0.7. The resulting mixture is stirred in an ultrasonic bath for 6 h at room temperature and then filtered using a 200-nm-diameter sterile syringe filter (Corning Inc., NY) to remove particulate materials. Twelve percent (w/w) PDLLA precursor is prepared by dissolving an appropriate number of PDLLA pellets into chloroform at room temperature. The mixture was stored at 4 °C for 24 h to dissolve these pellets fully and then vigorously stirred to obtain a transparent, homogeneous solution.

**Selective Surface Patterning of SAMs.** Photocleavable SAM technology is used to pattern the hydrophobic and hydrophilic regions on the collector surface (Figure 2a−d). The details of this technology are described in ref 30. Briefly, a glass slide surface is flushed with a mixture of 0.5% (w/w) octadecyltrichlorosilane (OTS) in hexadecane to form a hydrophobic SAM. The SAM surface is rinsed with hexane and methanol sequentially and then dried using nitrogen. Ultraviolet (365 nm) light is used to expose the SAM surface through a photomask in the pH 11.6 NaOH environment for 85 min. The UV-irradiated surface becomes hydrophilic, and the unirradiated one remains

(29) Titanium (50 nm) and gold thin films (200 nm) are first evaporated onto 1 in. × 3 in. glass slides (Corning Inc., NY). The titanium layer serves to improve the adhesion between gold and the glass slide. Then, photoresist AZ 5214E is spin-coated onto the slide at 4000 rpm for 40 s. After the prebake treatment in an oven at 85 °C for 30 min, UV light with an intensity of 7.5 mW/cm$^2$ is used to expose the photoresist through a photomask for 30 s. Subsequently, the slide is soaked in MIF-300 developer for 90 s to thoroughly remove unwanted photoresist. The postbake treatment is conducted in an oven at 120 °C for 30 min to stabilize the photoresist. Finally, a wet etching method is used to etch the unwanted gold and titanium, which involves (i) soaking the slide in a 1% (w/w) hydrofluoric acid solution for 4 min, (ii) soaking the slide in a gold etchant GE8148 solution (Transene Inc., MA) for 1 min, and (iii) thoroughly washing away the remaining photoresist using acetone and methanol sequentially and drying in air.

(30) Zhao, B.; Moore, J. S.; Beebe, D. J. *Science* **2001**, *291*, 1023–1026.

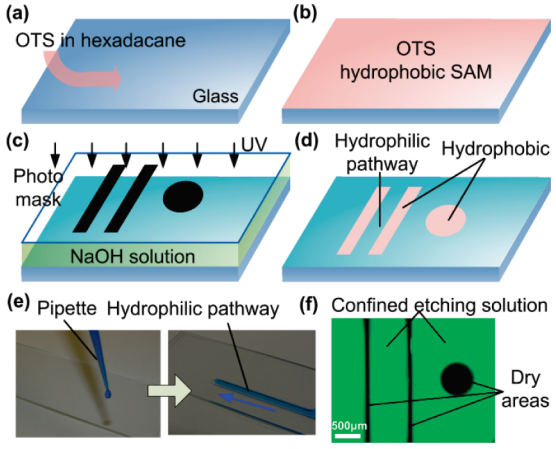


**Figure 2.** Process for modifying the collector surface using the photocleavable SAM technology and microfluidic filling. (a, b) The OTS hydrophobic SAM is formed on the glass surface. (c, d) The hydrophilic regions are patterned under UV light through the photomask. The gap between the glass surface and photomask is filled with NaOH solution. (e) The water/acetone etching solution (W/A = 50/50 w/w) is allowed to flow into the hydrophilic region via microfluidic filling. (f) Fluorescence image of the water/acetone mixture (W/A = 50/50 w/w) confined to the hydrophilic region.

hydrophobic. As a result, water-containing fiber-etching solutions can be confined to the hydrophilic region (Figure 2f).

**Microfluidic Capillary Filling and Confinement of Fiber-Etching Solution.** Deionized (DI) water is chosen to etch unwanted PEO fibers in the hydrophilic region. Although a number of organic solvents are available to dissolve water-insoluable PDLLA, they usually cannot be confined to the hydrophilic region themselves. To solve this problem, a mixture of water and a water-soluble organic solvent with a mixing ratio of water/acetone (or W/A) = 50/50 w/w is used to etch unwanted PDLLA fibers. (See the optimization of W/A in the Results and Discussion section.) The flow of the etching solution into the hydropilic region is realized through a simple microfluidic filling process (Figure 2). Placing a properly sized droplet of the etching solution in a liquid access port using a conventional pipet is all that is needed to start the flow of etching solution into the hydrophilic region. In this process, the capillary force of the droplet serves to drive the etching solution along the hydrophilic pathway. Figure 2e shows the flowing and confining process of the etching solution on the collector surface.

**Electrospinning of Fibers.** The PEO and PDLLA precursors are loaded into 10-mm-diameter syringes A and B, respectively. A no. 30 gauge stainless steel needle (Howard Electronic Instruments Inc.) is connected to a dc high-voltage supply (Gamma High Voltage Research Inc.). A syringe pump (model KDS210, $K_d$ Scientific Inc.) is used to deliver the precursor to the needle with a certain distance between the needle tip and the collector surface. The electrospinning conditions for PEO are listed as follows: the voltage applied between the needle tip and fiber collector is $V_{SC}$ = 6 kV, the distance between the needle top and fiber collector is $D$ = 10 cm, and the flow rate of the precursor is FR = 0.2 mL/h. For electrospinning of PDLLA, the following process conditions are used: $V_{SC}$ = 9 kV, $D$ = 12 cm, and FR = 0.5 mL/h.

**Scanning Electron Microscope (SEM) Observation.** The fiber diameter and mat thickness are measured using an SEM (SEM-JEOL JSM 606LV). Samples are sputtered with gold before observation. The distribution of fiber diameters (mean value ± standard deviation) is obtained by random sampling and the measurement of 80 individual fibers. To analyze the distribution of mat thicknesses, samples are cut carefully to expose their cross sections. Fifteen cross-section SEM images are taken to calculate the statistical value of the mat thickness.

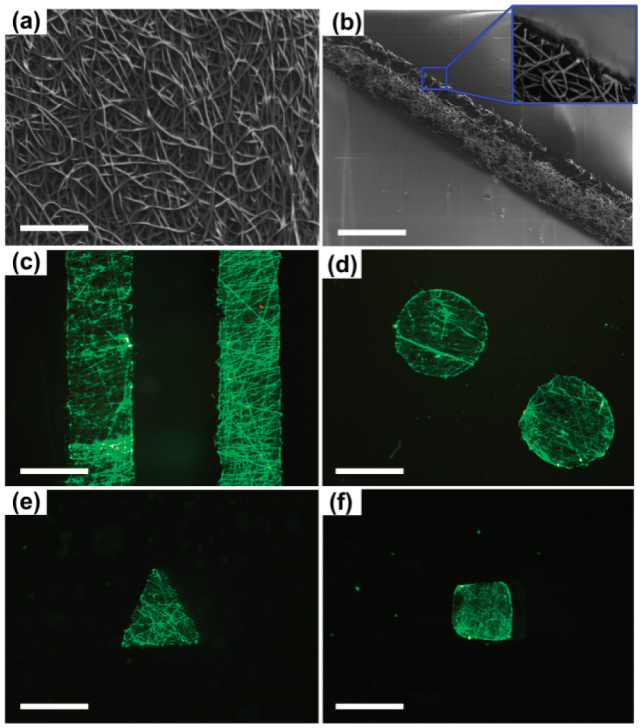


**Figure 3.** (a) SEM image of the as-electrospun PDLLA fibers. The scale bar represents 10 μm. (b) SEM image of the patterned PDLLA fiber belt. The inset shows the edge of the belt. Fluorescence images of the (c, d) PDLLA and (e, f) PEO nanofiber patterns with various shapes. Scale bars in b−f represent 50 μm.

**Contact Angle Measurement.** The contact angle wetting test is performed with a goniometer (OCA-20, DataPhysics Instruments GmbH, Germany). A drop of fluid is placed on the surface modified using photocleavable SAM technology. The image of the profile of the drop is taken by the goniometer. The contact angles are calculated by the accompanying SCA-20 commercial software (DataPhysics Instruments GmbH, Germany). The distribution of contact angles is achieved through the measurement of 10 droplets on each surface.

## Results and Discussion

The fabricated PEO and PDLLA fibers are 500 ± 120 and 930 ± 196 nm in diameter, respectively. Photocleavable SAM technology results in contact angles of DI water of 0 and 109 ± 1.2° on the hydrophilic and hydrophobic surfaces, respectively. The contact angles of the water/acetone mixture (W/A = 50/50 w/w) are found to be 0 and 59 ± 1.5° on the hydrophilic and hydrophobic surfaces, respectively. As expected, both of the etching solutions are successfully confined to the hydrophilic regions. The PEO and PDLLA fibers are observed to dissolve completely in pure water and the water/acetone mixture, respectively. To remove the remaining polymer residues from the hydrophilic surface, the surface is gently washed through a careful flowing and withdrawing process of the etching solution again (DI water for removing the PEO residues and a mixture of acetone and water with W/A = 50/50 w/w for removing the PDLLA residues).

Figure 3 shows the obtained fiber patterns using the presented selective nanofiber deposition method. A small amount of fluorescein dye is added to the fiber precursors to improve the visualization of the microstructures. It is clear that almost all the PEO and PDLLA residues are removed from the hydrophilic regions because no fluorescence is observed from the peripheral regions of the fibers. These patterns have high definition, and their

feature sizes are several tens of micrometers, almost one order higher than those obtained using most other methods[12−25] and comparable to that achieved using expensive femtosecond laser microchining.[28]

The selective nanofiber deposition method can incorporate with some nanofiber alignment techniques to obtain micropatterns in well-aligned fiber mats. We have demonstrated the selective deposition of aligned nanofibers by using a pair of electrodes[1] on the surface of the microfluidic collector. As shown in Figure 4, two parallel gold electrodes are first formed on the glass slide surface using the conventional microfabrication technology.[29] The hydrophobic and hydrophilic regions are then created between the two electrodes, followed by flowing the etching solution into the hydrophilic region. Such a spatial configuration results in suitable electrostatic forces that stretch the charged polymer jet to span across the gap and align perpendicular to the electrodes during electrospinning.[1] Therefore, the aligned nanofibers are deposited selectively on the surface of the hydrophobic region. The aligning direction of the nanofibers can be readily adjusted by changing the angle of the parallel electrodes with respect to the hydrophobic and hydrophilic patterns (Figure 4). The ability to deposit aligned nanofibers selectively in discrete areas could benefit the definition of the preferred direction of cell motion.

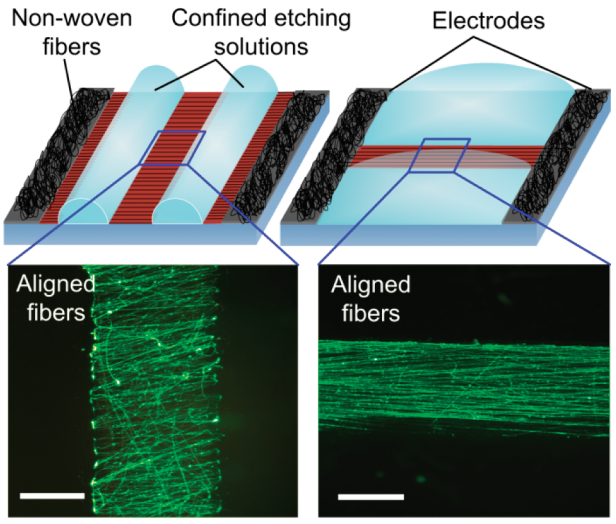


**Figure 4.** Selective deposition of aligned nanofibers on the collector surface. The hydrophilic and hydrophobic patterns are formed between two microfabricated parallel gold electrodes. The scale bars represent 50 $\mu$m.

Because of the inherent porous structure and large surface area of the fiber mat, the fiber-etching solution has a fairly high chance to laterally penetrate and overetch the nanofibers deposited in the hydrophobic region. The final patterns of the nanofibers always have smaller dimensions than those designed on the photomask. The amount of lateral overetch, however, can be compensated for by an increase in the dimensions of the pattern designed on the photomask. Therefore, it is important to identify and understand the possible factors that determine the lateral overetch. In the following section, we will discuss the influences of the composition of etching solution, electrospinning conditions, fiber diameter, and mat thickness on the lateral overetch and shape definition of fibers.

The introduction of DI water into a proper organic solvent allows the confinement of the etching solution to the hydrophilic region for etching water-insoluble nanofibers but at the same time decreases the etching ability of the etching solution. A trade-off thus exists between the confining property and etching ability of the etching solution. In this study, the former is characterized by the contact angle of the etching solution on the hydrophilic surface, and the latter is characterized by the etching time, which refers to the time from completing electrospinning to the visual clearance of the nanofibers in the hydrophilic region. Figure 5a shows the contact angles $\theta$ and corresponding etching times of the

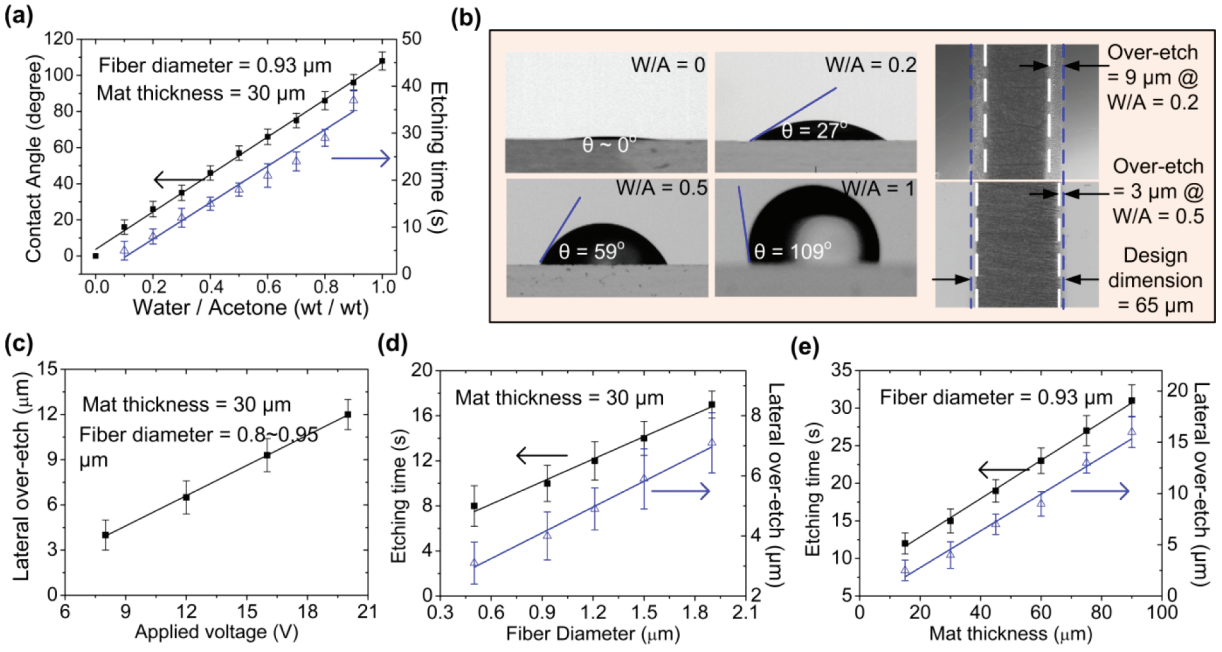


**Figure 5.** (a) Dependences of the contact angles of the water/acetone mixtures (left axis) and the time required to etch PDLLA fibers (right axis) on the W/A mixing ratio, respectively. (b) Left and middle columns show the optical images of the water/acetone droplets with W/A = 0:1, 0.2:0.8, 0.5:0.5, and 1:0 (w/w), respectively, placed on the hydrophilic surface formed via photocleavable SAM technology. The right column shows the lateral overetch at the edges of the PDLLA patterns (fiber diameter = 930 ± 196 nm; mat thickness = 30 ± 7 $\mu$m). (c) Dependence of the lateral overetch of the PDLLA fibers on the voltage applied at the spinneret. (d, e) Dependence of the etching time and the lateral overetch on (d) the PDLLA fiber diameter and (e) the mat thickness, respectively. Error bars represent ±SD.

water/acetone mixtures with different W/A ratios. Here, $\theta$ is found to increase linearly with increasing W/A ratio. The etching solution with a small $\theta$ or low W /A ratio is weakly confined to the hydrophilic region, and a slight perturbation (e.g., impingement of nanofibers onto the etching solution) can cause the etching solution to cross the hydrophobic−hydrophilic contact line and hence overetching the nanofibers deposited in the hydrophobic region. The resulting patterned area of nanofibers is thus reduced. (See the image in the upper right corner of Figure 5b.) As $\theta$ increases with decreasing acetone content, the etching time becomes longer. The optimum W/A ratio is found to range from 40/60 to 60/40 w/w, and the corresponding $\theta$ ranges from $48 \pm 4.1$ to $65 \pm 3.3°$. Specifically, at W/A = 50/50 w/w, the time required to etch the PDLLA fibers (fiber diameter = $930 \pm 196$ nm; mat thickness = $30 \pm 7$ $\mu$m) is $17 \pm 1.8$ s and the lateral overetch is only about 3 $\mu$m. (See the image in the bottom right corner of Figure 5b.)

The voltage potential, $V_{SC}$, applied between the needle tip and collector is another important factor in influencing the lateral overetch. As the charged jet moves closer to the collector during electrospinning, it achieves acceleration because of the increasing electrostatic force. At a high voltage $V_{SC}$, the impingement force from the traveling jet onto the etching solution destroys the confinement of the etching solution. Consequently, the etching solution invades the fiber-deposition region, resulting in a low-definition shape of nanofibers. Figure 5c shows the lateral overetch at the edges of the PDLLA patterns as a function of $V_{SC}$. At $V_{SC}$ = 20 kV, the lateral overetch is pronounced. Lowering $V_{SC}$ to 8 kV reduces the overetching effect.

Both the fiber diameter $d$ and mat thickness $h$ also affect the lateral overetch at the edges of the fiber patterns. It is observed that in the case of the selective deposition of large-diameter fibers the etching solution penetrates deeply into the patterned region along the fibers that do not melt immediately, causing severe overetching of the fibers. $d$ is found to rely significantly on the polymer concentration in the precursor solution. As the PDLLA concentration changes from 7.5 to 20% (w/w), $d$ increases linearly from $500 \pm 110$ to $1920 \pm 395$ nm. Fibers with $d = 500 \pm 110$, $930 \pm 196$, $1210 \pm 258$, $1550 \pm 320$, and $1920 \pm 395$ nm are electrospun onto five microfluidic collectors, respectively. The etching solution used here has a mixing ratio of W/A = 50/50 w/w. The result shows that the lateral overetch increases linearly with increasing $d$ (Figure 5d). A plausible explanation of this observation is given as follows. First, large-diameter fibers require a longer etching time to melt completely than do small-diameter fibers under the same etching conditions, thus more etching solution penetrates into the dry hydrophobic region along the large-diameter fibers, causing more lateral overetching. Second, large-diameter fibers carry more weight, hence hitting the etching solution harder and interrupting the equilibrium state of the etching solution more seriously than do the small-diameter ones. The consequent serious vibration of the etching solution causes a large amount of lateral overetching. As for the mat thickness, PDLLA fiber mats with $h = 18 \pm 4$, $30 \pm 7$, $44 \pm 12$, $60 \pm 16$, $75 \pm 19$, and $90 \pm 23$ $\mu$m are formed on six microfluidic collectors and patterned using the water/acetone mixture (W/A = 50/50 w/w). Figure 5e shows that the amount of lateral overetching is almost linear with respect to mat thickness. It is easy to understand that the thicker the fiber mat, the larger the contact area between the fiber mat and etching solution in the vertical direction and thus the more the etching solution invades the fiber-deposition region laterally. Therefore, large amounts of lateral overetching are observed during the selective deposition of thick fiber mats. In addition, it is found that given a constant mat thickness, the fiber mat composed of small-diameter fibers is more porous than that composed of large-diameter fibers, hence requiring a shorter etching time under the same etching conditions.

The presented selective nanofiber deposition method is fairly simple, and the minimum requirements are the creation of the hydrophilic and hydrophobic regions on the collector surface and the confinement of the water-containing organic etching solution in the hydrophilic region. Besides the PEO and PDLLA nanofibers, many other types of nanofibers (e.g., polymethylmethacrylate, polydimethylsiloxane, polyvinylchloride, and polystyrene) can be selectively deposited on glass substrates using this method. Water-miscible polar organic solvents (e.g., acetonitrile, acetic acid, ethanol, dimethylformamide, ethanol, and 2-propanol) are preferred in preparing the aqueous etching solutions; some nonpolar organic solvents with acceptable SW (e.g., dimethylsulfoxide, SW = 25 g/100 g; tetrahydrofuran, SW = 30 g/100 g; and 2-butanone, SW = 26 g/100 g) can also be used.[31] Therefore, the wide selection of organic solvents ensures that the selective deposition of a broad range of nanofibers can be processed with a minor modification to the composition of the etching solution.

## Conclusions

A novel, selective nanofiber deposition method is presented to realize the formation of microsized, structurally accurate, arbitrarily shaped patterns of both random and aligned nanofibers. The method involves using a unique microfluidic collector where the water-containing fiber-etching solution is selectively confined to defined regions by means of photocleavable SAM technology. Nanofibers accumulate on the hydrophobic (dry) surface and dissolve in the etching solution confined to the wet region. The photocleavable SAM technology offers apparent simplicity and flexibility in defining the hydrophilic and hydrophobic regions to realize the confinement of the etching solution. Through the microfluidic capillary filling process, the etching solution can flow into the hydrophilic region conveniently. The presented selective nanofiber deposition technology could lead to new application opportunities in cell biology and tissue engineering by producing high-definition shapes of electrospun nanofibers.

**Acknowledgment.** We thank Professor Donald S. Sakaguchi of the Department of Genetics, Development and Cell Biology, and Mr. Depeng Mao and Ms. Pooja Ramesh of the Department of Electrical and Computer Engineering at the Iowa State University for discussions. This work is partially supported by the U.S. DOE's Ames Laboratory Seed Fund.

(31) Reichardt, C. *Solvents and Solvent Effects in Organic Chemistry*, 3rd ed.; Wiley-VCH: Weinheim, Germany, 2003.